

國立臺灣大學理學院天文物理所

博士論文

Department of Computer Science and Information Engineering

College of Electrical Engineering and Computer Science

National Taiwan University

Doctoral Thesis

新的保守量與原始量的轉換法於狹義相對論性流體力
學並使用高速圖形顯示卡於自適性網格

An adaptive mesh, GPU-accelerated, and error minimized
special relativistic hydrodynamics code

曾柏勳

Po-Hsun Tseng

指導教授：闕志鴻博士

Advisor: Tzihong Chiueh, Ph.D.

中華民國 111 年 6 月

June, 2022

國立臺灣大學博士學位論文

口試委員會審定書

新的保守量與原始量的轉換法於狹義相對論性流
體力學並使用高速圖形顯示卡於自適性網格

An adaptive mesh, GPU-accelerated, and error
minimized special relativistic hydrodynamics code

本論文係曾柏勳君 (D05244001) 在國立臺灣大學天文物理所
完成之博士學位論文，於民國 111 年 6 月 28 日承下列考試委員審
查通過及口試及格，特此證明

口試委員：

<hr/>	
<hr/>	<hr/>
<hr/>	<hr/>
<hr/>	<hr/>
<hr/>	<hr/>

所 長：

<hr/>

誌謝

感謝...

Acknowledgements

I'm glad to thank. . .

摘要

本論文提出了一影像中使用者感興趣區域 (region of interest) 偵測之資料集 (benchmark)。使用者感興趣區域偵測在許多應用中極為有用，過去雖然有許多使用者感興趣區域之自動偵測演算法被提出，然而由於缺乏公開資料集，這些方法往往只測試了各自的小量資料而難以互相比較。從其它領域可以發現，基於公開資料集的可重製實驗與該領域突飛猛進密切相關，因此本論文填補了此領域之不足，我們提出名為「Photoshoot」的遊戲來蒐集人們對於感興趣區域的標記，並以這些標記來建立資料集。透過這個遊戲，我們已蒐集大量使用者對於感興趣區域的標記，並結合這些資料成為使用者感興趣區域模型。我們利用這些模型來量化評估五個使用者感興趣區域偵測演算法，此資料集也可更進一步作為基於學習理論演算法的測試資料，因此使基於學習理論的偵測演算法成為可能。

關鍵字： 相對論性流體演算法、費米氣泡、義羅西塔氣泡

Abstract

We present a new special relativistic hydrodynamics (SRHD) code capable of handling coexisting ultra-relativistically hot and non-relativistically cold gases. We achieve this by designing a new algorithm for conversion between primitive and conserved variables in the SRHD solver, which incorporates a realistic ideal-gas equation of state covering both the relativistic and non-relativistic regimes. The code can handle problems involving a Lorentz factor as high as 10^6 and optimally avoid the catastrophic cancellation. In addition, we have integrated this new SRHD solver into the code `GAMER` (<https://github.com/gamer-project/gamer>) to support adaptive mesh refinement and hybrid OpenMP/MPI/GPU parallelization. It achieves a peak performance of 7×10^7 cell updates per second on a single Tesla P100 GPU and scales well to 2048 GPUs. We apply this code to two interesting astrophysical applications: (a) an asymmetric explosion source on the relativistic blast wave and (b) the flow acceleration and limb-brightening of relativistic jets.

Keywords: relativistic jets, numerical method

Contents

口試委員會審定書	iii
誌謝	v
Acknowledgements	vii
摘要	ix
Abstract	xi
1 Introduction	1
Part I	3
2 Special relativistic hydrodynamics	5
2.0.1 Relativistic hydrodynamics	5
2.0.2 Equations of state	7
2.0.3 Conversion between primitive and conserved variables	10
Bibliography	15

List of Figures

- 2.1 The effective adiabatic index Γ (top left), the reduced enthalpy $\tilde{h}/c^2 := h/c^2 - 1$ (top right) as a function of temperature. Bottom panels show that Equation (2.10) approaches Equation (2.9) in both high- and low- T limits, where the maximum relative errors $1 - \Gamma_{\text{TM}}/\Gamma_{\text{exact}}$ and $1 - \tilde{h}_{\text{TM}}/\tilde{h}_{\text{exact}}$, are only 1.9 and 2.0 per cent, respectively. 9
- 2.2 Numerical errors of the conversion from conserved to primitive variables as a function of \mathcal{M} and $k_B T/mc^2$. The top and middle panel show the errors of the new and original schemes estimated by Equation (2.20) and Equation (2.21), respectively. The bottom panel shows the ratio of Equation (2.21) to Equation (2.20). ?? in Appendix ?? provides numerical evidences showing a remarkable consistency with the predicted values at $k_B T/mc^2 = 10^{-8}$ (blue dashed-dotted line). 13

List of Tables

Chapter 1

Introduction

Many high energy astrophysical problems involve relativistic flows. The problems include, for example, collimated jets in active galactic nuclei (AGN) (Chiueh et al. 1991; Li et al. 1992; Blandford et al. 2019), collapsar models of long-duration gamma-ray bursts [Woosley, 1993], magnetized relativistic winds and nebulae from pulsars (Kennel and Coroniti 1984a; Kennel and Coroniti 1984b; Chiueh 1989; Chiueh et al. 1998), and mildly relativistic wide-angle outflows in neutron star mergers (Mooley et al. 2018a; Mooley et al. 2018b; Ghirlanda et al. 2019; Fong et al. 2019). The full scope of these problems generally involves substantial temperature changes between jets (winds) and ambient gases. For this reason, the pioneering works of Taub [1948], Mathews [1971], and Mignone et al. [2005] suggested Taub-Mathews equation of state (TM EoS) that approximates the exact EoS [Synge, 1957] for ultra-relativistically hot (high- T hereafter) gases coexisting with non-relativistically cold (low- T hereafter) gases.

In addition, Noble et al. [2006] first compared the accuracy of several schemes for recovering primitive variables in the Riemann problems by means of self-checking tests (see Appendix ?? for details). Mignone and McKinney [2007] further proposed an inversion scheme for an arbitrary EoS and suggested that directly evolving the reduced energy density (i.e. the energy density subtracting the rest mass energy density from the total energy density) can avoid catastrophic cancellation in the non-relativistic limit. However, very few studies have systematically investigated how serious the catastrophic cancellation bears upon simulation results. This is partially due to the lack of exact

solutions with which numerical results can be compared.

In this paper, we propose a new numerical scheme for conversion between primitive and conserved variables in the presence of both high- T and low- T gases. The new scheme is carefully tailored to avoid catastrophic cancellation. To verify its accuracy, we numerically derive the exact solutions of two relativistic Riemann problems with the TM EoS and compare with the simulation results. It demonstrates that our new special relativistic hydrodynamics (SRHD) code can minimize numerical errors compared with conventional methods.

We have integrated this new SRHD solver into the code `GAMER` (Schive et al. 2010; Schive et al. 2018) to facilitate GPU acceleration and adaptive mesh refinement (AMR). This new code, `GAMER-SR`, yields good weak and strong scalings using up to 2048 GPUs on `Piz-Daint`, the supercomputer at the Swiss National Supercomputing Centre (CSCS). Finally, we present two astrophysical applications, an asymmetric explosion and self-accelerating jets, to demonstrate the capability of this new code in extreme conditions. All simulation data are analysed and visualized using the package `yt` [Turk et al., 2011].

This paper is organized as follows. We introduce the equation of state and our new scheme for conversion between primitive and conserved variables in Section ???. In Section ??, we describe numerical methods, including the AMR structure, GPU acceleration, flexible time-steps, and correction of unphysical results. In Sections ?? and ??, we conduct numerical experiments to demonstrate the accuracy in both the non-relativistic (NR) and ultra-relativistic (UR) limits, the performance scalability, as well as the limitation of `GAMER-SR`. Finally, we present two astrophysical applications in Section ?? and draw the conclusion in Section ??.

Note that the speed of light and the Boltzmann constant are hard-coded to 1 in `GAMER-SR`. However, these physical constants are retained in this paper, except in Appendices, for dimensional consistency.

Part I

Special relativistic hydrodynamics

Chapter 2

Special relativistic hydrodynamics

2.0.1 Relativistic hydrodynamics

Mass and energy-momentum conservation laws of a special relativistic ideal fluid follow

$$\partial_\nu (\rho U^\nu) = 0, \quad (2.1a)$$

$$\partial_\nu T^{\mu\nu} = 0, \quad (2.1b)$$

where

$$T^{\mu\nu} = \rho h U^\mu U^\nu / c^2 + p \eta^{\mu\nu}. \quad (2.2)$$

ρ and p are the proper mass density and the pressure, U^μ the four-velocity, $\eta^{\mu\nu}$ the metric tensor of Minkowski space, and c the speed of light. h is the specific enthalpy, related to the specific thermal energy ϵ by

$$h = c^2 + \epsilon + \frac{p}{\rho}. \quad (2.3)$$

An equation of state, $h(\rho, p)$, is required to close Equation (2.1) and will be discussed in Section 2.0.2. Throughout this paper, lower-case Greek indices run from 0 to 3, Latin ones from 1 to 3, and the Einstein summation convention is used, except when stated otherwise.

Equation (2.1) can be rewritten into a convenient conservative form for numerical

integration:

$$\partial_t D + \partial_j (DU^j / \gamma) = 0, \quad (2.4a)$$

$$\partial_t M^i + \partial_j (M^i U^j / \gamma + p \delta^{ij}) = 0, \quad (2.4b)$$

$$\partial_t E + \partial_j (M^j c^2) = 0, \quad (2.4c)$$

where γ is the Lorentz factor, and δ^{ij} is the Kronecker delta notation.

The five conserved quantities D , M^i , and E are the mass density, the momentum densities, and the total energy density, respectively. All conserved variables are related to primitive variables (ρ, U^i, p) through

$$D = \rho \gamma, \quad (2.5a)$$

$$M^i = D h U^i / c^2, \quad (2.5b)$$

$$E = D h \gamma - p. \quad (2.5c)$$

Nevertheless, Mignone and McKinney [2007] suggest evolving the reduced energy density,

$$\tilde{E} := E - D c^2, \quad (2.6)$$

instead of the total energy density; otherwise, extraction of a tiny thermal energy for a cold gas from the total energy will lead to catastrophic cancellation. An intuitive approach is to subtract Equation (2.4a) from Equation (2.4c) so that we can obtain a new energy equation. However, the new energy flux, $(M^j - DU^j / \gamma) c^2$, also suffers from catastrophic cancellation in the NR limit. An appropriate new energy flux avoiding such a problem is $(\tilde{E} + p) U^j / \gamma$, which is mathematically equivalent to $(M^j - DU^j / \gamma) c^2$. The reduced energy equation for numerical integration can thus be cast into

$$\partial_t \tilde{E} + \partial_j [(\tilde{E} + p) U^j / \gamma] = 0, \quad (2.7)$$

which is to replace Equation (2.4c).

Moreover, solving the Lorentz factor γ as three-velocity ($v = \sqrt{v^i v_i}$) approaches c can seriously suffer from catastrophic cancellation when using $\gamma = 1/\sqrt{1 - v^i v_i/c^2}$. Therefore, we explicitly adopt four-velocities (U^i) instead of three-velocity (v^i) for numerical computations and solve the Lorentz factor in terms of four-velocities as

$$\gamma = \sqrt{1 + U^i U_i/c^2}, \quad (2.8)$$

by which significant digits in γ can be kept when $\gamma \gg 1$.

In addition, unlike the three-velocity bounded by c , four-velocity U^i has no upper limit and therefore can greatly reduce the risk of having $v > c$ due to numerical errors.

2.0.2 Equations of state

GAMER-SR supports two kinds of EoS, the Taub-Mathews EoS (TM; Taub 1948, Mathews 1971, Mignone et al. 2005) and the polytropic EoS with a constant ratio of specific heats Γ . Assuming an ideal fluid in local thermal equilibrium and obeying the non-degenerate Maxwell-Jüttner statistics [Jüttner, 1911], the exact EoS [Synge, 1957] derived from the kinetic theory of relativistic gases is given by

$$\frac{h_{\text{exact}}}{c^2} = \frac{K_3 (mc^2/k_B T)}{K_2 (mc^2/k_B T)}, \quad (2.9)$$

where k_B and T are the Boltzmann constant and temperature, respectively, and K_n the n -th order modified Bessel function of the second kind. However, direct use of Equation (2.9) is computationally inefficient because the evaluation of Bessel function is numerically expensive.

Alternatively, the TM EoS is an approximation of Equation (2.9) and given by

$$\frac{h_{\text{TM}}}{c^2} = 2.5 \left(\frac{k_B T}{mc^2} \right) + \sqrt{2.25 \left(\frac{k_B T}{mc^2} \right)^2 + 1}. \quad (2.10)$$

The effective Γ can be found by equating Equation (2.9) or Equation (2.10) to the

polytropic EoS,

$$\frac{h_\Gamma}{c^2} = 1 + \frac{\Gamma}{\Gamma - 1} \left(\frac{k_B T}{mc^2} \right), \quad (2.11)$$

and solving Γ for the exact or TM EoS, respectively. As depicted in Figure 2.1, the maximum relative errors $1 - \Gamma_{\text{TM}}/\Gamma_{\text{exact}}$ and $1 - \tilde{h}_{\text{TM}}/\tilde{h}_{\text{exact}}$ are found to be only 1.9 and 2.0 per cent, respectively. In addition, Equation (2.10) approaches Equation (2.9) in both high- and low- T limits. Detailed comparisons between Equation (2.9) and Equation (2.10) have been presented previously (Mignone et al. 2005; Ryu et al. 2006; Mignone and McKinney 2007) and we do not repeat here.

On the other hand, the polytropic EoS has the advantage of simplicity and therefore has been used in many SRHD codes, such as FLASH [Fryxell et al., 2000], CAFE [Lora-Clavijo et al., 2015], and XTROEM-FV [Núñez-de la Rosa and Munz, 2016]. However, the polytropic EoS cannot handle the case where relativistic gases and non-relativistic gases coexist, primarily because the ratio of specific heats depends sensitively on temperature when $k_B T \sim mc^2$ (see the upper left panel in Figure 2.1). Moreover, the polytropic EoS with a non-relativistic $\Gamma = 5/3$ and a relativistic $\Gamma = 4/3$ does not satisfy the Taub's fundamental inequality for ideal gases [Taub, 1948]

$$\left[\frac{h}{c^2} - \left(\frac{k_B T}{mc^2} \right) \right] \left[\frac{h}{c^2} - 4 \left(\frac{k_B T}{mc^2} \right) \right] \geq 1, \quad (2.12)$$

implying that Γ must lie between $4/3$ and $5/3$ for any positive and finite value of temperature. Although the polytropic EoS is physically incorrect, we still reserve this feature in GAMER-SR for fast computation of a pure non-relativistic or relativistic gas.

The other two important quantities are the Mach number (\mathcal{M}) and the sound speed (c_s), given by

$$\mathcal{M} = \frac{\sqrt{U^i U_i}}{U_s}, \quad (2.13)$$

and

$$\frac{c_s}{c} = \sqrt{\frac{k_B T/mc^2}{3h/c^2} \left(\frac{5h/c^2 - 8k_B T/mc^2}{h/c^2 - k_B T/mc^2} \right)}, \quad (2.14)$$

for the TM EoS, where $U_s = c_s/\sqrt{1 - (c_s/c)^2}$. The sound speed approaches $c/\sqrt{3}$ at

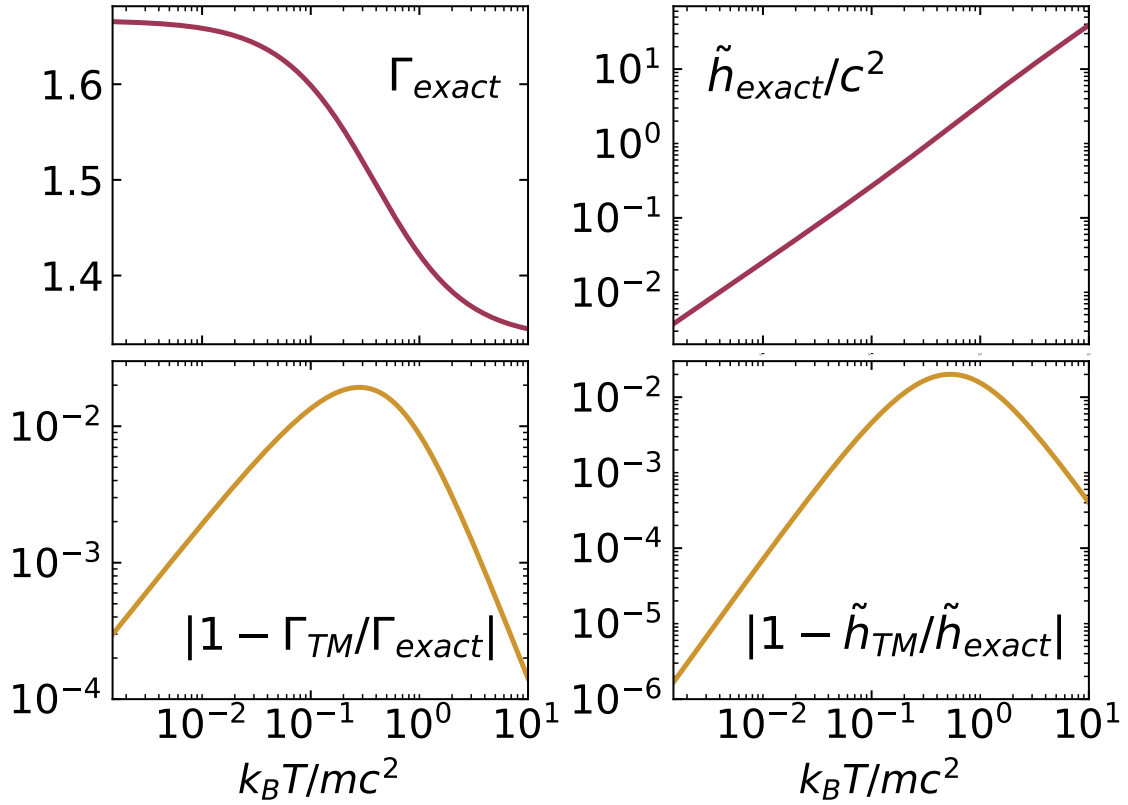


Figure 2.1: The effective adiabatic index Γ (top left), the reduced enthalpy $\tilde{h}/c^2 := h/c^2 - 1$ (top right) as a function of temperature. Bottom panels show that Equation (2.10) approaches Equation (2.9) in both high- and low- T limits, where the maximum relative errors $1 - \Gamma_{TM}/\Gamma_{exact}$ and $1 - \tilde{h}_{TM}/\tilde{h}_{exact}$, are only 1.9 and 2.0 per cent, respectively.

ultra-relativistic temperature and will be used in the Riemann solver.

2.0.3 Conversion between primitive and conserved variables

In standard Riemann-type numerical schemes, conversion between conserved and primitive variables is a common procedure for data reconstructions and flux computations. For non-relativistic hydrodynamics, this conversion can be carried out in a straightforward and analytical manner. However, designing an accurate and efficient conversion algorithm for a relativistic problem in the presence of NR gases, which involves root-finding, is challenging. This is because catastrophic cancellations may arise in the non-relativistic gas.

Here we propose a new conversion scheme to solve this problem based on the TM EoS. The reduced energy density (Equation 2.6) and the momentum density (Equation

2.5b) satisfy the relation

$$\begin{aligned}
& \left(\frac{\tilde{E}}{Dc^2} \right)^2 + 2 \left(\frac{\tilde{E}}{Dc^2} \right) - \left(\frac{\mathbf{M}}{Dc} \right)^2 \\
&= \frac{\tilde{h}^2}{c^4} + \frac{2\tilde{h}}{c^2} - 2 \left(\frac{k_B T}{mc^2} \right) \left(\frac{\tilde{h}}{c^2} + 1 \right) + \frac{(k_B T/mc^2)^2 (\tilde{h} + c^2)^2}{(\tilde{h} + c^2)^2 + \left(\frac{Mc}{D} \right)^2} \\
&:= f(\tilde{h}),
\end{aligned} \tag{2.15}$$

where f is positive definite, $\tilde{h} := h - c^2$ is the reduced enthalpy, and the temperature $k_B T/mc^2$ is related to \tilde{h} by inverting Equation (2.10):

$$\frac{k_B T}{mc^2} = \frac{2(\tilde{h}/c^2)^2 + 4(\tilde{h}/c^2)}{5(\tilde{h}/c^2) + 5 + \sqrt{9(\tilde{h}/c^2)^2 + 18(\tilde{h}/c^2) + 25}}. \tag{2.16}$$

The conserved variables \tilde{E} , M^j , and D on the left-hand side are known quantities updated at every time step, from which one can solve for \tilde{h} .

We adopt $\tilde{h} = h - c^2$ instead of h as the root because the latter is dominated by rest mass energy density in the low- T limit and thus will suffer from catastrophic cancellation when numerically extracting temperature from trailing digits.

Equation (2.15) is suitable for the Newton-Raphson iteration method as it is a monotonically increasing function of \tilde{h} . That is, Equation (2.15) has no zero derivative of \tilde{h} that might otherwise lead to a divergence of the iterative procedure. The Newton-Raphson method requires an initial guess of \tilde{h} and the derivative of Equation (2.15) for iteration, both of which are presented in Appendix ???. We adopt the convergence criterion $1 - \tilde{h}_i/\tilde{h}_{i+1} \leq \epsilon_{\text{machine}}$, where \tilde{h}_i is the approximate root at the i th iteration and $\epsilon_{\text{machine}}$ is the machine precision (10^{-7} and 10^{-16} for single and double precision, respectively).

After obtaining \tilde{h} , we substitute it into Equation (2.5b) to get four-velocity:

$$U^i = \frac{M^i c^2}{D(c^2 + \tilde{h})}. \tag{2.17}$$

Next, we compute the Lorentz factor and proper mass density from Equation (2.8) and Equation (2.5a) and then use Equation (2.16) to obtain temperature. Finally, the pressure

is given by

$$p = \rho c^2 \left(\frac{k_B T}{mc^2} \right). \quad (2.18)$$

Justifying the superiority of our new conversion scheme using \tilde{E} , we estimate the relative error of computing $a - b$ by [Higham, 2002]

$$\frac{|a| + |b|}{|a - b|} \epsilon_{\text{machine}}. \quad (2.19)$$

Thus, the error of the new conversion scheme can be estimated by substituting $\left[(\tilde{E}/Dc^2)^2 + 2(\tilde{E}/Dc^2) \right]$ and $(\mathbf{M}/Dc)^2$ for a and b , respectively, in Equation (2.19). The error in terms of primitive variables reads

$$\begin{aligned} & \left[\frac{\gamma^2 (\tilde{h} + 1)^2 (1 + \beta^2) + \frac{T^2}{\gamma^2} - 2(\tilde{h} + 1)T - 1}{(\tilde{h} + 1)^2 + \frac{T^2}{\gamma^2} - 2(\tilde{h} + 1)T - 1} \right] \epsilon_{\text{machine}} \\ & \approx (1 + \mathcal{M}^2) \epsilon_{\text{machine}}, \end{aligned} \quad (2.20)$$

where $\beta = \sqrt{v^i v_i}/c$. The approximate equality in Equation (2.20) holds for all finite temperature.

According to Equation (2.13) and Equation (2.20), we can decide whether to adopt single or double precision before simulations. Taking ultra-relativistic pulsar wind ($\mathcal{M}_{\text{wind}} \approx 10^6$) as an example, we must use double precision to suppress the error to 10^{-4} . But for mild-relativistic AGN jets ($\mathcal{M}_{\text{jet}} < 10$), single precision is sufficient to reduce the error to 10^{-5} .

For the original scheme using the total energy density E instead of \tilde{E} , a similar error estimation can be performed by replacing \tilde{E} with $E - Dc^2$ on the left-hand side of Equation (2.15), which gives

$$\left[\frac{2\gamma^2 (\tilde{h} + 1)^2 + \frac{T^2}{\gamma^2} - 2(\tilde{h} + 1)T + (\tilde{h} + 1)^2 + 1}{(\tilde{h} + 2)\tilde{h} + \frac{T^2}{\gamma^2} - 2(\tilde{h} + 1)T} \right] \epsilon_{\text{machine}}. \quad (2.21)$$

Figure 2.2 shows the contour plots of Equation (2.20) for the new scheme (top panel) and Equation (2.21) for the original scheme (middle panel) as a function of \mathcal{M} and

temperature. The bottom panel shows the ratio of Equation (2.21) to Equation (2.20). It demonstrates the advantage of using \tilde{E} . The top panel shows that using \tilde{E} in the conversion scheme is almost error-free when dealing with subsonic flows at any finite temperature, including the low- T limit. In supersonic flows, the numerical errors proportional to \mathcal{M}^2 are common and caused by finite digits of floating numbers. In comparison, the middle panel shows the error using E , which severely suffers from catastrophic cancellation in the low- T limit even when $\mathcal{M} \ll 1$. See also ?? in Appendix ??.

On the other hand, conversion from primitive to conserved variables is also needed in the Riemann solver. This procedure involves straightforward substitution without the need of root-finding. We use

$$\frac{\tilde{h}}{c^2} = 2.5 \left(\frac{k_B T}{mc^2} \right) + \frac{2.25 (k_B T / mc^2)^2}{1 + \sqrt{2.25 (k_B T / mc^2)^2 + 1}}, \quad (2.22)$$

and

$$\frac{\tilde{E}}{Dc^2} = \frac{\left(\frac{\mathbf{M}}{Dc} \right)^2 + f(\tilde{h})}{1 + \sqrt{1 + \left(\frac{\mathbf{M}}{Dc} \right)^2 + f(\tilde{h})}}, \quad (2.23)$$

to compute \tilde{h} and \tilde{E} , where $f(\tilde{h})$ can be computed from Equation (2.15) with known \mathbf{M}/Dc . Note that Equation (2.22) and Equation (2.23), following directly from Equation (2.10) and Equation (2.15) without any approximation, are written in a form without any subtraction to avoid catastrophic cancellation. In contrast, using Equation (2.5c) and Equation (2.6) to compute the reduced energy density \tilde{E} can suffer from catastrophic cancellation in the NR limit.

We close this section by providing a flowchart of the new conversion scheme in ?? in Appendix ?? and by summarizing the equations actually solved by GAMER-SR. Other mathematically equivalent forms are unrecommended as they may suffer from catastrophic cancellation in the UR or NR limit.

- Evolution equations: Equation (2.4a, 2.4b, 2.7).
- Lorentz factor: Equation (2.8).

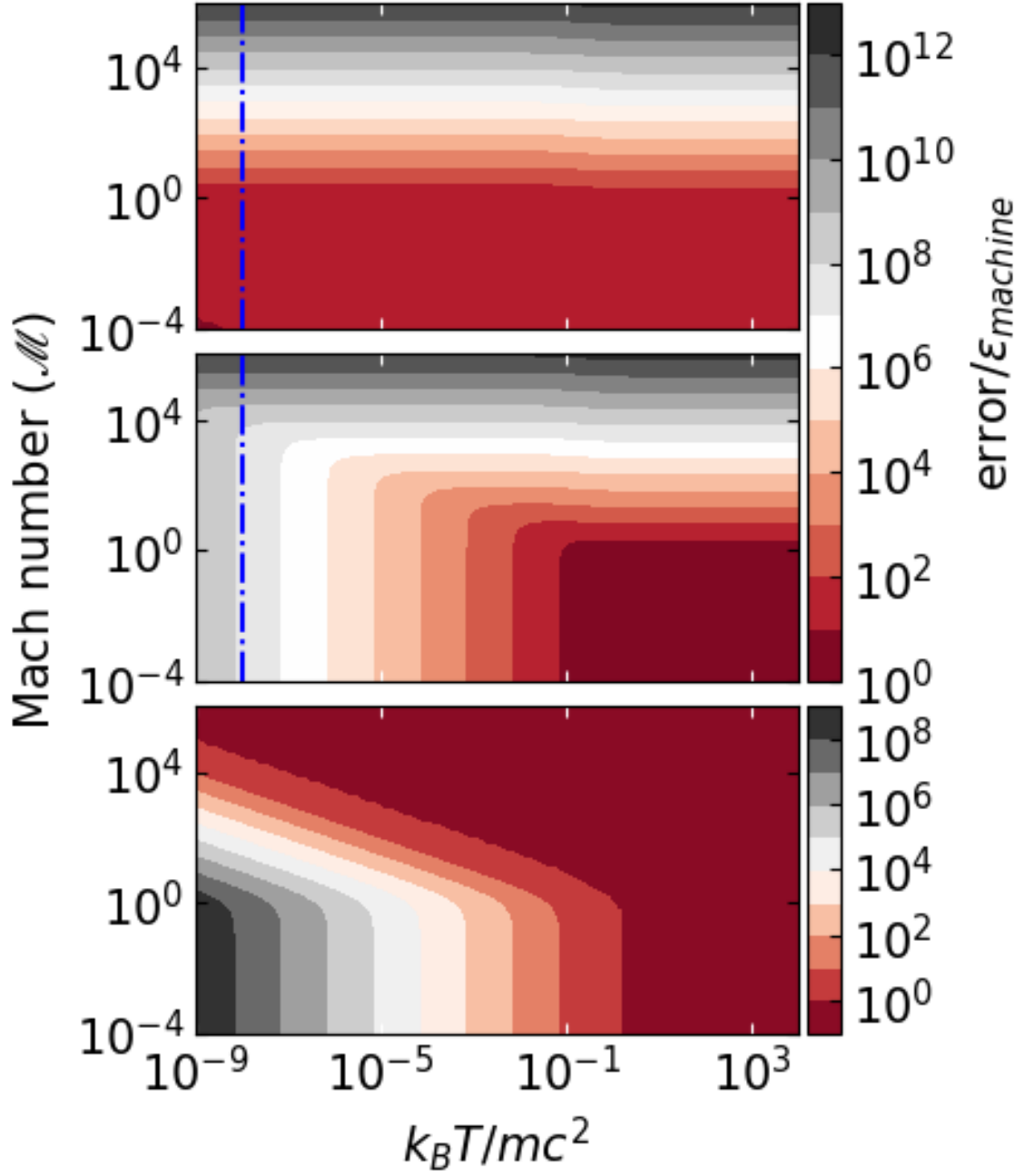


Figure 2.2: Numerical errors of the conversion from conserved to primitive variables as a function of \mathcal{M} and $k_B T / m c^2$. The top and middle panel show the errors of the new and original schemes estimated by Equation (2.20) and Equation (2.21), respectively. The bottom panel shows the ratio of Equation (2.21) to Equation (2.20). ?? in Appendix ?? provides numerical evidences showing a remarkable consistency with the predicted values at $k_B T / m c^2 = 10^{-8}$ (blue dashed-dotted line).

- Four-velocities: Equation (2.17).
- Temperature: Equation (2.16).
- Pressure: Equation (2.18).
- Reduced enthalpy: Equation (2.22).
- Reduced energy density: Equation (2.23).

Bibliography

- R. Blandford, D. Meier, and A. Readhead. Relativistic jets from active galactic nuclei. *Annual Review of Astronomy and Astrophysics*, 57(1):467–509, 2019. . URL <https://doi.org/10.1146/annurev-astro-081817-051948>.
- T. Chiueh. Relativistic solitons and shocks in magnetized $e^-e^+p^+$ fluids. *Phys. Rev. Lett.*, 63:113–116, Jul 1989. . URL <https://link.aps.org/doi/10.1103/PhysRevLett.63.113>.
- T. Chiueh, Z.-Y. Li, and M. C. Begelman. Asymptotic Structure of Hydromagnetically Driven Relativistic Winds. , 377:462, Aug. 1991. .
- T. Chiueh, Z.-Y. Li, and M. C. Begelman. A critical analysis of ideal magnetohydrodynamic models for crab-like pulsar winds. *The Astrophysical Journal*, 505(2):835–843, oct 1998. . URL <https://doi.org/10.1086%2F306209>.
- W. Fong, P. K. Blanchard, K. D. Alexander, J. Strader, R. Margutti, A. Hajela, V. A. Villar, Y. Wu, C. S. Ye, E. Berger, R. Chornock, D. Coppejans, P. S. Cowperthwaite, T. Eftekhari, D. Giannios, C. Guidorzi, A. Kathirgamaraju, T. Laskar, A. Macfadyen, B. D. Metzger, M. Nicholl, K. Paterson, G. Terreran, D. J. Sand, L. Sironi, P. K. G. Williams, X. Xie, and J. Zrake. The Optical Afterglow of GW170817: An Off-axis Structured Jet and Deep Constraints on a Globular Cluster Origin. , 883(1):L1, Sept. 2019. .
- B. Fryxell, K. Olson, P. Ricker, F. X. Timmes, M. Zingale, D. Q. Lamb, P. MacNeice, R. Rosner, J. W. Truran, and H. Tufo. FLASH: An adaptive mesh hydrodynamics code for

- modeling astrophysical thermonuclear flashes. *The Astrophysical Journal Supplement Series*, 131(1):273–334, nov 2000. . URL <https://doi.org/10.1086%2F317361>.
- G. Ghirlanda, O. S. Salafia, Z. Paragi, M. Giroletti, J. Yang, B. Marcote, J. Blanchard, I. Agudo, T. An, M. G. Bernardini, R. Beswick, M. Branchesi, S. Campana, C. Casadio, E. Chassande-Mottin, M. Colpi, S. Covino, P. D’Avanzo, V. D’Elia, S. Frey, M. Gawronski, G. Ghisellini, L. I. Gurvits, P. G. Jonker, H. J. van Langevelde, A. Melandri, J. Moldon, L. Nava, A. Perego, M. A. Perez-Torres, C. Reynolds, R. Salvaterra, G. Tagliaferri, T. Venturi, S. D. Vergani, and M. Zhang. Compact radio emission indicates a structured jet was produced by a binary neutron star merger. *Science*, 363(6430):968–971, Mar. 2019. .
- N. J. Higham. *Accuracy and Stability of Numerical Algorithms*. Society for Industrial and Applied Mathematics, USA, 2nd edition, 2002. ISBN 0898715210.
- F. Jüttner. Das maxwellsche gesetz der geschwindigkeitsverteilung in der relativtheorie. *Annalen der Physik*, 339(5):856–882, 1911. . URL <https://onlinelibrary.wiley.com/doi/abs/10.1002/andp.19113390503>.
- C. F. Kennel and F. V. Coroniti. Confinement of the Crab pulsar’s wind by its supernova remnant. , 283:694–709, Aug. 1984a. .
- C. F. Kennel and F. V. Coroniti. Magnetohydrodynamic model of Crab nebula radiation. , 283:710–730, Aug. 1984b. .
- Z.-Y. Li, T. Chiueh, and M. C. Begelman. Electromagnetically Driven Relativistic Jets: A Class of Self-similar Solutions. , 394:459, Aug. 1992. .
- F. D. Lora-Clavijo, A. Cruz-Osorio, and F. S. Guzmán. CAFE: A NEW RELATIVISTIC MHD CODE. *The Astrophysical Journal Supplement Series*, 218(2):24, jun 2015. . URL <https://doi.org/10.1088%2F0067-0049%2F218%2F2%2F24>.
- W. G. Mathews. The Hydromagnetic Free Expansion of a Relativistic Gas. , 165:147, Apr 1971. .

- A. Mignone and J. C. McKinney. Equation of state in relativistic magnetohydrodynamics: variable versus constant adiabatic index. *Monthly Notices of the Royal Astronomical Society*, 378(3):1118–1130, 06 2007. ISSN 0035-8711. . URL <https://doi.org/10.1111/j.1365-2966.2007.11849.x>.
- A. Mignone, T. Plewa, and G. Bodo. The piecewise parabolic method for multidimensional relativistic fluid dynamics. *The Astrophysical Journal Supplement Series*, 160, 09 2005. .
- K. P. Mooley, A. T. Deller, O. Gottlieb, E. Nakar, G. Hallinan, S. Bourke, D. A. Frail, A. Horesh, A. Corsi, and K. Hotokezaka. Superluminal motion of a relativistic jet in the neutron-star merger GW170817. , 561(7723):355–359, Sept. 2018a. .
- K. P. Mooley, E. Nakar, K. Hotokezaka, G. Hallinan, A. Corsi, D. A. Frail, A. Horesh, T. Murphy, E. Lenc, D. L. Kaplan, K. de, D. Dobie, P. Chand ra, A. Deller, O. Gottlieb, M. M. Kasliwal, S. R. Kulkarni, S. T. Myers, S. Nissanke, T. Piran, C. Lynch, V. Bhalerao, S. Bourke, K. W. Bannister, and L. P. Singer. A mildly relativistic wide-angle outflow in the neutron-star merger event GW170817. , 554(7691):207–210, Feb. 2018b. .
- S. C. Noble, C. F. Gammie, J. C. McKinney, and L. D. Zanna. Primitive variable solvers for conservative general relativistic magnetohydrodynamics. *The Astrophysical Journal*, 641(1):626–637, apr 2006. . URL <https://doi.org/10.1086%2F500349>.
- J. Núñez-de la Rosa and C.-D. Munz. XTROEM-FV: a new code for computational astrophysics based on very high order finite-volume methods - II. Relativistic hydro- and magnetohydrodynamics. , 460(1):535–559, Jul 2016. .
- D. Ryu, I. Chattopadhyay, and E. Choi. Equation of state in numerical relativistic hydrodynamics. *The Astrophysical Journal Supplement Series*, 166(1):410–420, sep 2006. . URL <https://doi.org/10.1086%2F505937>.
- H.-Y. Schive, Y.-C. Tsai, and T. Chiueh. GAMER: A GRAPHIC PROCESSING UNIT ACCELERATED ADAPTIVE-MESH-REFINEMENT CODE FOR ASTROPHYSICS.

- The Astrophysical Journal Supplement Series*, 186(2):457–484, feb 2010. . URL <https://doi.org/10.1088%2F0067-0049%2F186%2F2%2F457>.
- H.-Y. Schive, J. A. ZuHone, N. J. Goldbaum, M. J. Turk, M. Gaspari, and C.-Y. Cheng. gamer-2: a GPU-accelerated adaptive mesh refinement code –accuracy, performance, and scalability. *Monthly Notices of the Royal Astronomical Society*, 481(4):4815–4840, 09 2018. ISSN 0035-8711. . URL <https://doi.org/10.1093/mnras/sty2586>.
- J. L. Synge. The Relativistic Gas. *North-Holland Pub. Co.; Interscience Publishers*, 1957.
- A. H. Taub. Relativistic Rankine-Hugoniot Equations. *Physical Review*, 74(3):328–334, Aug 1948. .
- M. J. Turk, B. D. Smith, J. S. Oishi, S. Skory, S. W. Skillman, T. Abel, and M. L. Norman. yt: A Multi-code Analysis Toolkit for Astrophysical Simulation Data. *The Astrophysical Journal Supplement Series*, 192:9, Jan. 2011. .
- S. E. Woosley. Gamma-Ray Bursts from Stellar Mass Accretion Disks around Black Holes. , 405:273, Mar. 1993. .